Validation of Radiation Dose from a four slice CT scanner using Monte Carlo

*Poonam Yadav[1,2,3], Velayudham Ramasubramanian[3]

[1]*Department of Human Oncology, University of Wisconsin, Madison, WI, USA*
[2]*Department of Medical Physics, University of Wisconsin, Madison, WI, USA*
[3]*Vellore Institute of Technology University, Vellore, Tamil Nadu, India*

_____

ABSTRACT

Objective: To simulate a computed tomography scanner using Monte Carlo code and validate it using standard dose measurements at the center and periphery of head and body phantom and to investigate the viability of gold foil as a dose enhancer in computed tomography scanning. Material and Methods: Head and body phantom of 16 cm and 32 cm diameter respectively with 16 cm length were used. A normalization factor to convert results to absolute dose values was obtained by simulations in air. The Monte Carlo N particle transport code was used to simulate standard dosimetric measurements. *Results: Measured and calculated values agree within 6%, with minor adjustable exceptions. The validated model is in accordance with the measured data. Also, the radiation dose is boosted by 6% when we applied the gold foils.*

Key Words: Computed Tomography, Computed Tomography Dose Index, Monte Carlo.

_____

INTRODUCTION

Computed Tomography (CT) is one of the most commonly used diagnostic procedures used in modern medicine. The population dose from CT procedures has escalated significantly in the last decade. It contributes a large percentage of radiation doses to the patients during medical procedure. Also, it is estimated that worldwide CT contributes 5% of the radiological examination and makes 34% contribution to the collective dose [1,2]. The application of CT scanner is continuing to increase with the widespread availability of multi detector CT scanner with faster gantry rotation time which improves spatial and temporal resolution of earlier scanners and has resulted in reduced examination time.

To determine the organ doses in CT examination is not a straightforward method. Presently, three dosimetric quantities are widely recognised in CT. These quantities are the volume computed tomography dose index ($CTDI_{vol}$, mGy), the dose length product (DLP, mGycm) and

472

the effective dose (E, mSv) respectively. They provide the radiation risk of the entire CT scan, average dose in the scanned region and the exposure from the complete CT examination. The concept of computed tomography doses index (CTDI) has been used over 25 years and is used to measure CT dose [3]. Since long time Monte Carlo simulation has predominated in determination of the organ dose in most fields of the radiation physics. The Monte Carlo method is a computational model in which physical quantities are calculated by simulating the transport of X-rays [4]. A Monte Carlo method is a computational algorithm which relies on repeated random sampling to compute its results. At present, Monte Carlo methods are widely used to solve a broad spectrum of problems in various areas of biomedical imaging, biochemistry, finance, geophysics, meteorology, computer application, public health studies, medical physics and many more. In radiological science Monte Carlo techniques have provided extremely valuable information through the simulation of radiation transport.

The aim of present study is to model a modern multislice CT scanner (Multislice medical CT scanner, ASTEION, super 4 edition, Toshiba and PMMA (polymethyl methacrylate) phantom, determine the $CTDI_w$ with the standard 100 mm pencil ionization chamber in air and PMMA phantom for all the range of beam collimations selectable in CT scanner for 80, 100, 120 and 135 kVp values experimentally and using Monte Carlo N-particle radiation transport computer code and compare the calculated and measured data. Finally the work was extended to study the dose difference in phantom with and without gold foils using the CT scanner. To verify the result from Monte Carlo, the dose was also calculated using thermoluminescent dosimeter (TLD) and the results were compared.

The validation of simulated model was carried out by observing the simulated $CTDI_{100}$ and $CTDI_W$ with corresponding measured $CTDI_{100}$ and $CTDI_W$ for different beam energies and slice thicknesses. The results were compared for both head and body phantoms.

MATERIALS AND METHODS

2.1. Overview of Monte Carlo
In our study, we have attempted to simulate the transport of photons in kilovoltage range to calculate scatter projections pertinent to diagnostic radiology CT scanners. There is wide range of avalibable Monte Carlo codes. Monte Carlo N-particle (MCNP) transport code is a general purpose, continuous energy, generalized geometry, time dependent code that can be used for neutron, photon, electron or coupled neutron/ photon/ electron transport and photon transport. The code takes into account photoelectric absorption, with the possibility of K and L shell fluorescent emission or Auger electron, coherent and incoherent scattering and pair production. The conventional modelling package is based upon a combinatorial geometry system using planes, cylinders, cones and spheres to define the geometry [5,6]. Also, it supports the nested lattice feature, for which user need to define the boundary cell, one lattice cell and the origin of the bounding cell. Thus, the repeated structure option provides the ability to simulate very complex and heterogeneous spatial activity distribution. The modelling requires the user to create an input file which contains all information about the geometry, components material composition details, form of result or tally and variance reduction techniques to be used. For all the experiment the number of histories was selected so that the relative dose remained as low as 1% [7].

473

2.2. CT model

The Toshiba multislice helical CT scanner (Asteion super 4 Edition) was used for all simulations. It is a third generation CT scanner equipped with solid state detectors system. The primary detectors are 788 channels × 22 elements and data acquisition detectors are 788 channels × 4 rows. Also, the model design consists of one pair of reference detectors. Scan time is 0.48 sec (partial); 0.75, 1, 1.5 (2 and 3) sec (360$^\bullet$). Scan time for full helical scan is 100 seconds. The slice thickness available are 1, 2, 3, 5, 7 and 10 mm and operating voltage are 80, 100, 120 and 135 kVp and the tube current can vary from 30 to 300 mAs in steps of 10 mAs. The nominal beam widths, i.e. the available beam collimations at the isocentre of the scanner, are determined by the N X h product, where number of slices acquired simultaneously is represented by N, and h denotes active detector width. Helical pitch can be set in the range from 2.5 to 8.0 in increments of 0.5 excluding 4.0 and pitch factor range is 0.625 to 2.0. Figure 1 shows the modelled multi detector design.
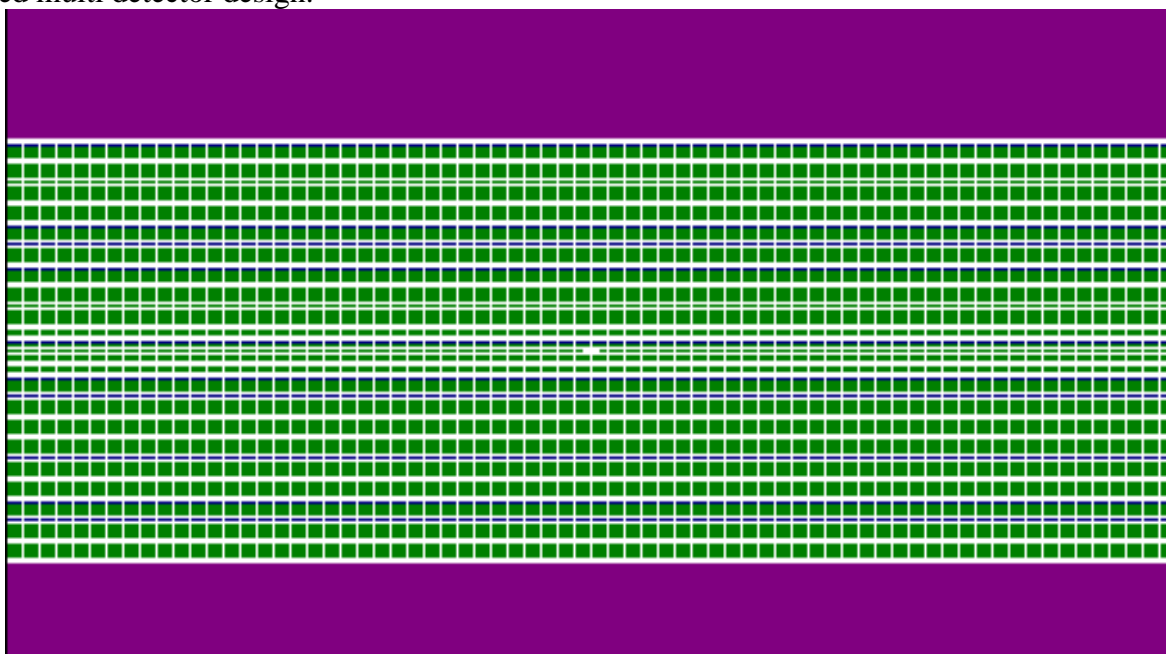

Figure 1: Multislice detector with 788 channel X 22 elements data acquisition detector model.

The distance from focal spot to the isocentre is 600 mm and the distance from focal spot to the detector is 1072 mm. The fan beam is collimated in the X-Y plane to a fan angle of 42.5$^\bullet$. The scanner has 22 rows of detectors; out of these, 22 rows middle four detectors have 0.5 mm thickness and other detector rows have 1 mm of thickness.

2.3. Phantom model

For this work, the standard body computed tomography dose index (CTDI) dosimetry phantom was used. The cylindrical phantom is 16 cm in length, and 16 cm and 32 cm in diameter for head and body, respectively. It is made of polymethyl-methacrylate (PMMA) with five sockets, one in the centre and other four at 1 cm from the phantom surface of about 1 cm in diameter were pencil ion chamber can be placed.
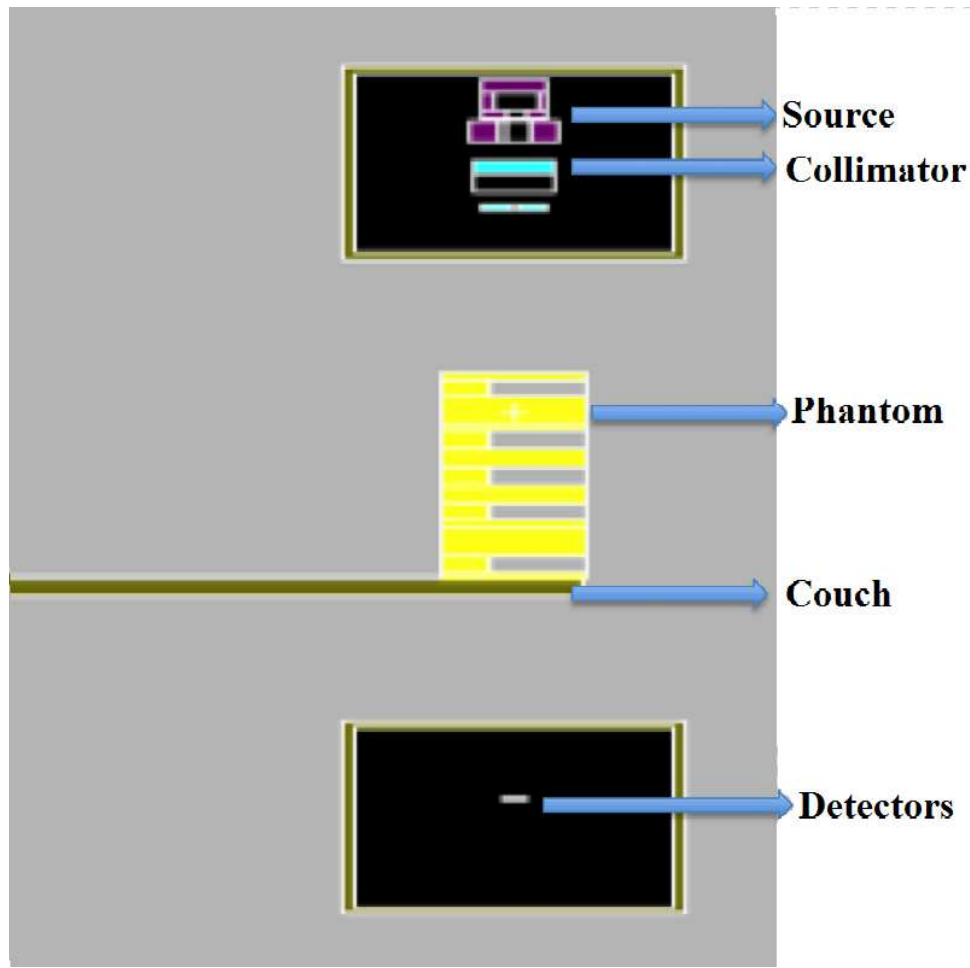
Figure 2: Modelled PMMA Phantom (in yellow colour) and system design. Upper part is source with collimator, slit and lower part is detector array.
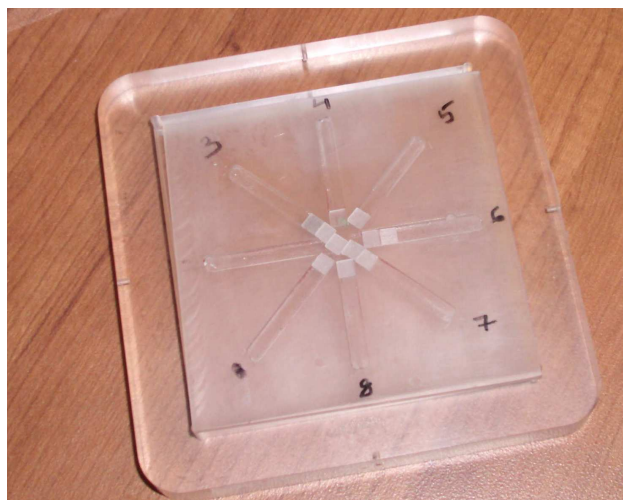

Figure 3: Experimental arrangement for gold foil and TLDs.

_____

2.3. Gold Foil and Acrylic slab

The work was further extended to place the gold foil, each of 1.3 cm in diameter and 0.05 mm in thickness in acrylic slab. These gold foils are embedded in between the two acrylic material slabs of length 6.3 cm, height 6.3 cm and thickness 2 mm. Experimental arrangement is shown in figure 3. This part of the experiment was done in order to compute the difference in dose with and without gold foil, and if there is good enhancement of the dose and then, can CT scanner be used for treatment apart from diagnosis.

Gold foils were chosen because of their high atomic number and also gold does not produce large toxicity in the human body. Overall, 24 TLDs were used for dose calculation and, the results of TLD were compared to the Monte Carlo based simulation results.

2.4. Measured Data

Two sets of reading were obtained. In the first set, exposures were acquired in air at the isocentre of the scanner for beam energies 80, 100, 120, 135 kVp for 10 mm slice thickness and for slice thickness 1, 2, 3, 5 and 7 mm at 120 kVp. For these measurements, a constant tube current of 100 mAs was used. The second set of reading were taken in PMMA phantom at the centre, 6:00 and 12:00 positions, the later two correspond to the anterior and posterior ion chamber locations, respectively. The CTDI was calculated keeping tube current 100 mA and other parameters same as explained above.

CTDI is defined as the integral along a line parallel to the axis of rotation (z) of the dose profile (D (z)) for a single rotation and a fixed couch position, divided by the nominal thickness of the x-ray beam. CTDI can be conveniently assessed using a pencil ionisation chamber with an active length of 100 mm, so as to provide a measurement of $CTDI_{100}$, expressed in terms of absorbed dose to air [8],

$$CTDI\ 100 = \frac{1}{N * T} \int_{-50}^{50} D(z)dz \qquad (1)$$

where N is the number of tomographic sections, each with a nominal thickness T (mm) from a single rotation. For multi-slice CT scanners, where N > 1, NxT (mm) represents the total detector acquisition width (e.g. 4 x 5 mm), and is equivalent to the nominal beam collimation.

Weighted CT dose index ($CTDI_W$) was calculated using following equation [9]:

$$CTDIw = \frac{2}{3}\ CTDIp\ |\ \frac{1}{3}\ CTDIc \qquad (2)$$

Where $CTDI_{100,p}$ represents an average of measurements at four equally-spaced locations around the periphery of the phantom.
The simulation based results were normalised using the formula:

$$(NF)E, T = \frac{(D\,air, measured)E, T}{(D\,air, simulated)E, T} \qquad (3)$$

Where, the denominator is the dose obtained by simulating ion chamber at the isocentre of scanner at beam energy E and slice thickness T and numerator is dose obtained at isocentre of scanner at 100 mAs, E energy and T slice thickness. Table 1, tabulates the normalized factors for converting the Monte Carlo results.

Table 1: Normalization factor for converting the Monte Carlo simulation results from mGy per source particle to mGy/100 mAs.

Beam Energy (kVp)	Slice Thickness (mm)	Measured CTDI$_{100}$ (mGy/100mAs)	Simulated CTDI$_{100}$ (mGy/100mAs)	Normalization Factor (10^{13} particles/mAs)
80	10	4.95	1.96×10^{-13}	2.53×10^{11}
100	10	11.57	2.92×10^{-13}	3.96×10^{11}
120	10	13.38	3.23×10^{-13}	4.12×10^{11}
135	10	15.92	4.41×10^{-13}	3.61×10^{11}
120	7	9.72	3.23×10^{-13}	3.01×10^{11}
120	5	7.41	3.23×10^{-13}	2.29×10^{11}
120	3	5.20	3.23×10^{-13}	1.61×10^{11}
120	2	4.32	3.23×10^{-13}	1.34×10^{11}
120	1	3.62	3.23×10^{-13}	1.12×10^{11}

It should be noted that the normalization factor is per mAs, so one has to multiply the simulated results by the normalization factor and total number of mAs to obtain absolute dose. Following equation is used for calculating the absolute dose [10,11]:

$$(D_{absolute})E,T = (N\,F)E,T \times (D_{simulated})\,E,T \times (Total\ mAs) \qquad (4)$$

Where $D_{simulated}$ is the simulated dose for energy E and slice thickness T. The simulated dose in phantom was calculated based upon an energy fluence tally and the mass energy absorption coefficients for acrylic. The measurements in air as well as in the simulated data were performed for various beam energies and slice thicknesses. Different normalization factors were obtained for different energies and slice thicknesses.

RESULTS

3.1. Part I: The measured and simulated CTDI$_{100}$ values in air at various energies and slice thicknesses are shown in Table 1. The CTDI$_{100}$ measurements were taken at tube current 100 mAs. The normalization factors were applied for converting simulated dose values to absolute dose values and were obtained uniquely for particular beam energy and slice thickness. The

477

measured and simulated CTDI$_{100}$ are shown in Table 2 and Table 3 respectively for head and body phantom at different points.

The result shows that both the methods are in consent within 6% at the periphery and 10% at the centre for head phantom, over all the slice thickness and beam energy settings. At low beam energies such as 80 kVp and 100 kVp, maximum percentage difference i.e. 9.6% and 5.4% at centre and periphery, respectively, is observed. In case of the body phantom the CTDI$_{100}$ has 6% difference at centre and 7% at periphery.

Table 2: Measured and Simulated CDTI$_{100}$ in the head phantom, as a function of beam energy and slice thickness

Position	Beam Energy (kVp)	Slice Thickness (mm)	Measured CTDI$_{100}$ (mGy/100 mAs)	Simulated CTDI$_{100}$ (mGy/100 mAs)	Percentage Difference (%)
6:00			5.97	6.13	2.610
Centre	80	10	4.23	4.68	9.615
12:00			7.81	7.41	-5.398
6:00			14.29	13.82	-3.400
Centre	100	10	13.42	14.20	5.493
12:00			15.37	16.15	4.830
6:00			23.31	23.92	2.550
Centre	120	10	24.44	25.38	3.704
12:00			26.81	25.76	-4.076
6:00			37.01	37.99	2.579
Centre	135	10	36.83	37.27	1.181
12:00			38.01	38.82	2.087
6:00			25.58	26.01	1.653
Centre	120	7	20.11	19.57	-2.759
12:00			22.97	23.26	1.247
6:00			26.98	26.19	-3.016
Centre	120	5	21.25	22.10	3.846
12:00			23.71	23.35	-1.542
6:00			27.39	27.99	2.144
Centre	120	3	23.47	22.17	-5.868
12:00			24.87	23.87	-4.189
6:00			28.86	29.12	0.893
Centre	120	2	24.17	24.67	2.027
12:00			25.79	26.12	1.263
6:00			29.21	28.95	-0.898
Centre	120	1	25.63	25.17	-1.828
12:00			26.15	26.79	2.389

Table 3: Measured and Simulated CDTI$_{100}$ in the body phantom as a function of beam energy and slice thickness

Position	Beam Energy (kVp)	Slice Thickness (mm)	Measured CTDI$_{100}$ (mGy/100 mAs)	Simulated CTDI$_{100}$ (mGy/100 mAs)	Percentage Difference (%)
6:00			2.19	2.24	2.232
Centre	80	10	1.57	1.61	2.484
12:00			4.31	4.59	6.100
6:00			6.54	6.21	-5.314
Centre	100	10	3.32	3.54	6.215
12:00			8.62	8.33	-3.481
6:00			18.73	17.67	-5.999
Centre	120	10	9.58	9.79	2.145
12:00			20.19	20.76	2.746
6:00			30.81	31.52	2.252
Centre	135	10	16.74	17.41	3.848
12:00			33.00	32.36	-1.977
6:00			16.79	17.35	3.228
Centre	120	7	10.05	10.42	3.551
12:00			18.41	19.29	4.562
6:00			16.91	17.67	4.301
Centre	120	5	10.62	10.08	-5.357
12:00			19.79	20.31	2.560
6:00			19.73	20.64	4.409
Centre	120	3	10.10	10.58	4.537
12:00			22.98	22.11	-3.935
6:00			20.11	20.71	2.897
Centre	120	2	10.13	10.08	-0.496
12:00			23.61	24.99	5.522
6:00			22.01	22.82	3.549
Centre	120	1	10.17	10.31	1.358
12:00			24.85	23.37	-6.333

3.2. Part II: The peripheral to centre dose was also computed. The results are shown in form of graph in Figure 4 and Figure 5 for head and body phantom separately, considering periphery values as average of values at 6 and 12 positions of phantom.

It is observed that the ratio of peripheral to central dose depend on the slice thickness and decreases with high voltage. In case of head phantom, the ratio varies in the range from 1.629 to 1.018 for measured dose and it ranges from 1.447 to 1.03 for simulated dose. In case of body phantom, the peripheral to central dose ratio varies from 1.68 to 2.34 for measured values and is in between from 1.2 to 2.27 for simulated values for body phantom; indeed this is wide range as compared to head phantom centre to periphery ratio.
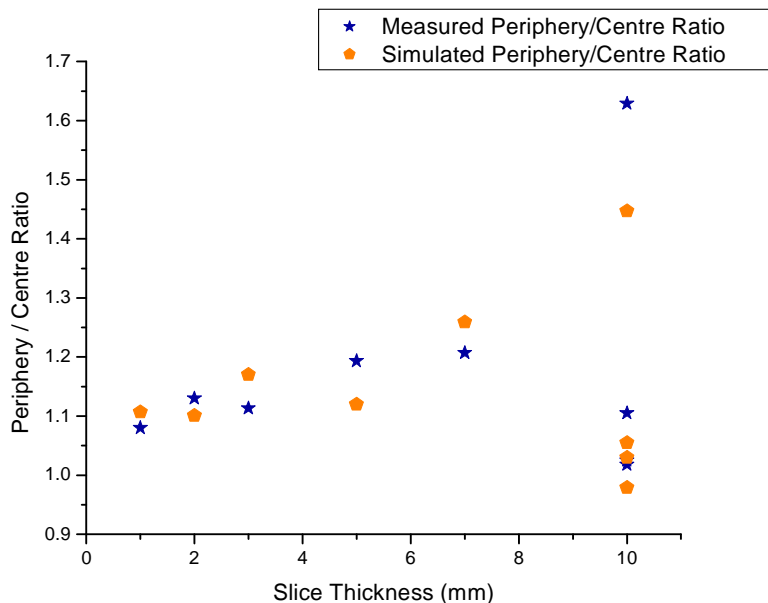
Figure 4: Comparison of measured and simulated periphery to centre ratio for head phantom at different slice thickness
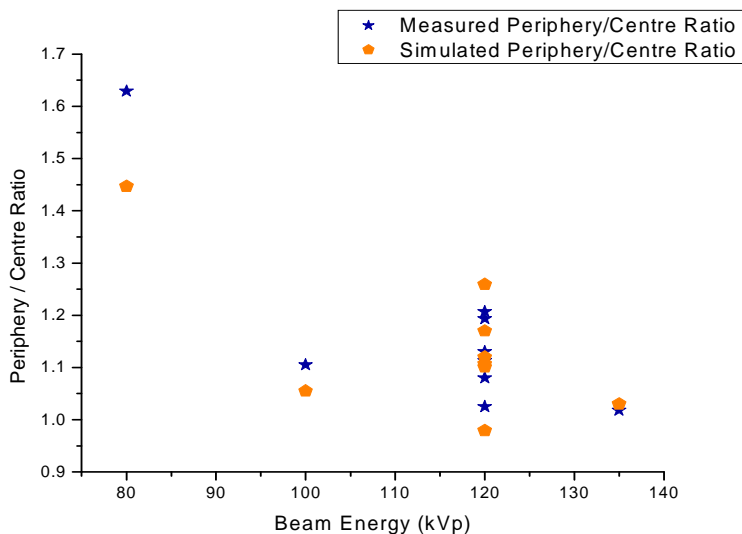

Figure 5: Comparison of measured and simulated periphery to centre ratio at different beam energy for head phantom.

3.3. Part III: $CTDI_W$ values were also computed with above illustrated setup and using equation 2 for head and body phantoms respectively. In case of head phantom $CTDI_W$ ranges from 6.00 to 37.28 and 6.07 to 38.03 for measured and simulated dose respectively with the difference ranging from -4% to 3%. In case of body phantom, $CTDI_W$ ranges from 2.69 to 26.85 and 1.82 to 27.1 for measured and simulated dose respectively, with the percentage difference ranging from -24% to 14%.

It is noticed that, the $CTDI_W$ increases with rise in beam energy keeping slice thickness and tube current constant, as shown in Table 6. Also, $CTDI_W$ rises though linearly with few exceptions, with reduction in slice thickness at constant beam energy and tube current for beam energy 120 kVp and tube current 100 mAs, while slice thickness varies from 1 mm to 10 mm.

480

Thus, there is undoubted dependence of $CTDI_W$ on slice thickness for beam energy 120 kVp and a wide variable range of slice thickness, as measured $CTDI_W$ varies up to 12.8% and 14.93% for head and body phantoms respectively, and simulated $CTDI_W$ raises up to 14.9% and 14.12% for head and body phantoms, respectively. There is little successive increase–decrease behaviour when all the constraints are put together. However, the CTDI values exhibited no monotonous pattern on beam collimation effect as observed in this investigation.

Table 6: Measured and simulated CTDI$_w$ for different beam energy and slice thickness for head and body phantom

Beam Energy (kVp)	Slice Thickness (mm)	For Head Phantom		For Body Phantom	
		CTDI$_w$ (Measured)	CTDIw (Simulated)	CTDIw (Measured)	CTDIw (Simulated)
80	10	6.00	6.07	2.69	1.82
100	10	14.36	14.72	6.16	6.03
120	10	24.85	25.02	16.17	16.07
135	10	37.28	38.03	26.85	27.10
120	7	22.89	22.95	15.08	15.69
120	5	23.98	23.88	15.77	16.02
120	3	25.24	24.68	17.60	17.78
120	2	26.27	26.64	17.95	18.60
120	1	26.01	26.97	19.01	18.83

3.4. Part IV: As we were satisfied with the model, we stepped further and set up an experimental arrangement to study the change in dose using gold foil in a phantom using a simple arrangement shown in Figure 6. The set up uses three acrylic slab, two of them were plain and one was designed to hold the TLD's and gold foil. The gold foil and TLD slab was pressed between the two plan slabs. The reason for using gold was a) it has a higher Z number than iodine (I, Z= 53) or gadolinium (Gd, Z = 64), b) it shows little toxicity, up to at least 3% by weight, on either the rodent or human tumor cells (Herold et al 2000).

Figure 6: Experimental arrangement for gold foil.

Because the atomic photoelectric cross-section is approximately proportional to Z4 ~ Z, the photoelectric interaction probability associated with a gold-loaded tumor, for example, is higher by at least a factor of 2 than that associated with a gadolinium loaded tumor, assuming same concentration of materials in the tumor and the same radiation quality. Thus, gold clearly leads to a higher tumor dose than either iodine or gadolinium. Table 7 shows that, there is enhancement in the dose for both TLD and MC calculation of 5.5 % and 6.7 % respectively for two gold foils. The two results agree within the range of 2.2%.

Table 7: TLD and MC reading comparison with and without gold foil

	TLD results mGy	*MC results mGy*	*Percentage Difference*
TLD	11.66	11.27	2.8
TLD + 2 Au foils	12.3	12.03	2.2
TLD + 4 Au foils	11.4	12.16	-6.6

It was also noted that there is not much increment in dose when 4 gold foils were used, though an increment is observed in the MC calculation. The Monte Carlo calculation was also repeated for 10 mm slice thickness. 6.3 % and 6.1 % of dose enhancement was observed for the 10 mm slice thickness in second and fourth gold foils, respectively. With high Z materials some low energy photons too, can produce photoelectrons which may be responsible for the dose enhancement.

DISCUSSION

The mean value $CTDI_W$ measured was 22.99 mGy which is close to mean value $CTDI_W$ simulated, which is 23.22 mGy for head phantom, and this difference agree within 1%, similarly for body phantom mean value $CTDI_W$ measured was 15.25 mGy which is near to mean value $CTDI_W$ simulated which is 15.33 mGy, with a percentage difference of 0.5%. The averages of measured $CTDI_{100}$ periphery and simulated $CTDI_{100}$ periphery are 18.31 mGy and 18.33 mGy and indeed exhibit good agreement. Also, these values shows considerable acceptance to $CTDI_w$

mean values which are 15.25 mGy and 15.33 mGy for measured and simulated values respectively, for body phantom. In case of head phantom, average $CTDI_{100}$ periphery are 23.89 mGy and 23.98 mGy for measured and simulated values respectively, and hence exhibits an affirmative difference of less than 0.4%. The corresponding values of $CTDI_w$ periphery for measured and simulated values are 22.99 mGy and 23.22 mGy respectively, and have difference of less than 1%. Hence, the results show accuracy in modelling. It is also observed that with decrease in kVp the simulated CTDI values tend to slightly overestimate the measured CTDI values. Random errors in the calculated dose may also contribute to the overall difference between measured and simulated values. Reduction in random error was attained by increasing the number of histories. It is also observed that $CTDI_W$ shows dependence on slice thickness.The ratio of peripheral to central dose depends on slice thickness and shows decreasing trend with high voltage. The ratios of peripheral to central doses show a smaller range in case of head phantom as compared to range of ratio in body phantom due to better penetration of radiation in case of head phantom.

The higher Z number and comparatively little toxicity are the prime reason and sufficient justifications for use of gold foil. Though the gold foils cannot be used in the real treatment, still the experiment was conducted to show that with low energy a good amount of dose enhancement can be achieved. So, we can say that CT in some cases can also be used for the treatment apart from the diagnosis. As the greatest challenge in radiation therapy is to deliver a lethal dose of radiation to a tumor while sparing nearby normal tissues and in pursuit of achieving this, gold can act as substantial dose enhancer.

REFERENCES

[1] P.C. Shrimpton; S. Edyvean; *Br J Radiol*, **1998**; 71: C1-3.

[2] M.R. Madan; B. Georg; K. Willi; G.J. Stephen; G. Lena; M. Takamichi; S. P. Shrimpton. Managing patient dose in computed tomography, International Commission on Radiological Protection (ICRP) publication 87, **2000**, 30(3), 1 -45.

[3] J.J. DeMarco1; C.H. Cagnon; D.D. Cody; D.M. Stevens; C.H. McCollough; J. O'Daniel; M. F. McNitt-Gray. **2005**, *Phys. Med. Biol*. 50(17), 3989–4004.

[4] J.W. Beck; W.L. Dunn; F. O'Foghludha., *Math. Phys*, **1983**, 10, 314–20.

[5] R.Y. Rubinstein. Simulation and the Monte Carlo Method (John Wiley & Sons), **1981**, 145-210.

[6] B.R.B. Walters; I. Kawrakow; D.W.O. Rogers. History by history statistical estimators in the BEAM code system, Med. Phys, **2002**, 29, 2745–2752.

[7] J.F. Briesmeister. MCNP—A General Monte Carlo N-Particle Transport Code, Report LA-12625-M. NM: Los Alamos National Laboratory, Los Alamos, **1997**, Version 4B.

[8] European commission, Quality criteria for computed tomography, European, EUR16262 (working document). Brussels: EC, **1997**.

[9] P.C. Shrimpton; M.C. Hillier; M.A. Lewis; M. Dunn. Doses from Computed Tomography (CT) Examination in the UK, **2003**, NRPB-W67.

[10] G. Jarry; J.J. DeMacro; U. Beifuss; C.H. Cagnon; M. F. McNitt-Gray. *Phys. Med. Bio*, **2003**, 48, 2645-2663.

[11] J.D. Gones; P.C. Shrimpton. Survey of CT practice in the UK. Part 3: normalised organ doses calculated using Monte Carlo techniques (NRPB-R250). Chilton: National Radiological Protection Board, **1991**.